



## Real-time analysis and classification of bioaerosols based on optical scattering properties

MIRON KALISZEWSKI<sup>1</sup>, ELŻBIETA ANNA TRAFNY<sup>1,2</sup>, MAKSYMILIAN  
WŁODARSKI<sup>1</sup>, RAFAŁ LEWANDOWSKI<sup>1,2</sup>, MAŁGORZATA STĘPIŃSKA<sup>1,2</sup>,  
MIROSLAW KWAŚNY<sup>1</sup>, JERZY KOSTECKI<sup>1</sup>, KRZYSZTOF KOPCZYŃSKI<sup>1</sup>

<sup>1</sup>Wojskowa Akademia Techniczna, Instytut Optoelektroniki,  
00-908 Warszawa, ul. gen. S. Kaliskiego 2

<sup>2</sup>Wojskowy Instytut Higieny i Epidemiologii, Zakład Mikrobiologii,  
01-163 Warszawa, ul. Kozielska 4, miron.kaliszewski@wat.edu.pl

**Abstract.** The size and shape of biological particles are important parameters allowing discrimination between various species. We have studied several aerosols of biological origin such as pollens, bacterial spores and vegetative bacteria. All of them presented different morphology. Using optical size and shape analyser we found good correlation between light scattering properties and actual particle features determined by scanning electron and fluorescence microscopy. In this study, we demonstrated that HCA (Hierarchical Cluster Analysis) offers fast and continuous bioaerosol classification based on shape and size data matrices of aerosols. The HCA gives an unequivocal interpretation of particle size vs. asymmetry data. Therefore, it may provide high throughput and reliable screening and classification of bioaerosols using scattering characteristics.

**Keywords:** bioaerosol classification, scattering, particle size and shape analysis, biological warfare agents' detection, hierarchical cluster analysis (HCA)

**DOI:** 10.5604/01.3001.0009.9475

### 1. Introduction

The morphological features, i.e. shape and size distribution are essential in classification of biological particles. These data could be significant in many areas of interest: environmental monitoring, climate research, and many industrial settings. Morphology of particles is also crucial in bioaerosol studies where the assessment

of number, viability and hazard, connected to the air transmission of harmful biological agents, is expected to erase real time alerts (Trafny et al. 2014).

The detection of bacteria in the air is a serious task, due to the relatively low concentration of vegetative bacterial cells and endospores and the complexity of biological particles in the air samples. During the last two decades, a several devices for single airborne particle monitoring have been developed (1-5). Their operating principle is based mainly on the fluorescence of intrinsic fluorophores that are excited with a laser.

The fluorescence does not provide sufficient information for clear and reliable identification of bacterial or fungal air-borne species. It allows only rough, however real-time, discrimination of potential battlefield man-made interferents from intentionally released biological warfare agents. Based on the intrinsic fluorescence, the air-borne bacteria can be classified using various approaches, as follows: the ratio of fluorescent particles, proportion of fluorescence measured in different spectral bands, Principal Component Analysis (PCA) and Hierarchical Cluster Analysis (HCA) (5-10). In our previous studies, we have applied various statistical approaches in order to better discriminate between bacteria, fungi, pollens, spores and natural interferents in outdoor and the laboratory-generated bioaerosols. The HCA approach (11) has significantly improved the biological agents' classification in the air samples comparing to the the previously used methods. However, the data are still lacking on whether the use of HCA analysis might advance the air-borne biological particles discrimination based on the ASAS (Aerosol Size and Shape) technology. The first commercial device developed by Kaye et al. (12) has been commercialized by Biral as an instrument called ASPECT (Biral Ltd., UK). The device uses three detectors for particle shape determination. They are arranged at 120° azimuthal offset that allows collection of scattered light intensity. The response of all three detectors enables the determination of asymmetry factor of each particle (13, 14).

In the available literature, only a few reports can be found on the the use of ASPECT detector for characterization of bacterial particles. The most recent paper concerning the ASPECT application described its ability to characterize the shape and size alteration of bacterial cells that underwent different heating conditions. This study did not intend to compare the scattering characteristics of air-borne bacteria and pollens (15). Nevertheless, bacteria and pollens are coexisting in the environment and it could lead to false classification. Therefore, the goal of our study was to assess the possibility of real time environmental monitoring with the use of the size and shape analysis of bioaerosols and statistical approach to data gathering and interpretation.

## 2. Materials and methods

### 2.1. Materials

The aerosols were generated from the dried biological and non-biological materials. Based on anthrax letters evidences, the aerosolization from dry powders should be expected in case of a potential bioterrorist attack (16). The materials used in this study are listed in Table 1, together with their abbreviations.

TABLE 1

Samples used in tests

Sample	Abbreviation	Source
B. atrophaeus spore	BGs	WIHE
M. Luteus	ML	WIHE
<i>B. thuringiensis</i> spores technical (Turex)	BTst	WIHE
<i>B. atrophaeus</i> spores technical	BGst	WIHE
Ragweed pollen	RAG	Duke Sci. Corp.
Johnson's grass smut spores	JONs	Duke Sci. Corp.
Polystyrene Latex Spheres 34-1 (3-8 µm)	PLS	Duke Sci. Corp.
Paper mulberry pollen	PAP	Duke Sci. Corp.

WIHE — Military Institute of Hygiene and Epidemiology, Warsaw, Poland.

### 2.2. Bacterial strains

The following reference Gram-positive bacterial strains *Bacillus atrophaeus* ATCC 9372 (BG) and *Micrococcus luteus* ATCC 4698 (ML) were purchased from the American Type Culture Collection (ATCC) and used in this study. Culturing of the bacterial strains and their subsequent storage was performed in accordance with procedures consistent with the requirements of the ATCC.

### 2.3. Freeze-drying bacteria

Bacterial lyophilizates, obtained from *Bacillus atrophaeus* var. *globigii* (BG) (ATCC 9372) spores or *Micrococcus luteus* (ATCC 4698) vegetative cells, were used in this study. BG strain was grown on a solid 2 SG sporulation medium and the endospores were purified and stored as described by Lewandowski et al. (17). BG endospores, suspended in sterile deionized water or *M. luteus* cells suspended in sterile saline solution, were freeze-dried in a Lyovac GT2 (Leybold GmbH, Germany) at maximum vacuum  $6 \times 10^{-1}$  mbar for 24 h. Before each experiment, the bacterial

lyophilizates were placed in a test chamber (glove box Model 830-ABB/Sp 800-HEPA/D, Plas-Labs, Inc., Lansing, MI, USA). The bacterial lyophilizates were then scraped from a bottom of the flasks using 28-cm Cell Scraper (Greiner Bio-One GmbH, Germany) and were hand-crushed in mortars. The minced microbiological materials were then transferred to RapidFlaem 6 (RF6) head (Flaem Nuova S.p.A, Brescia, Italy).

## 2.4. Bioaerosol experimental system

Bioaerosols were generated in a test chamber (an interior volume of  $0.5 \text{ m}^3$ ), which was placed in a laboratory room with exhaust ventilation. The BG endospores were aerosolized inside the chamber filled with a HEPA-filtered air. Bioaerosols were

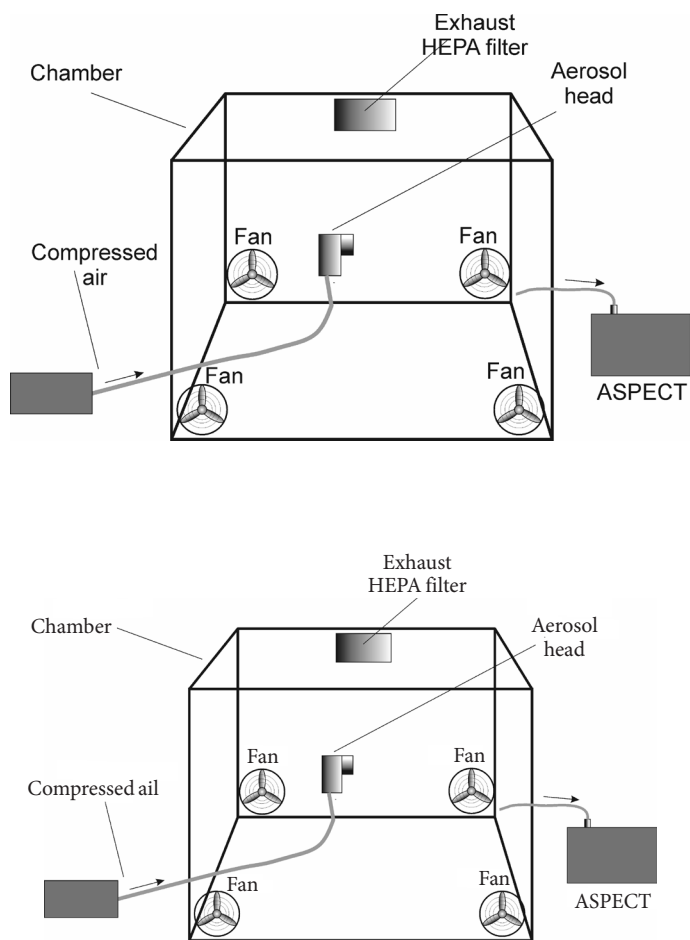


Fig. 1. Schematic diagram of experimental setup

generated by a compressed-air nebulizer Monsun 2 MP2 (Medbryt, Warsaw, Poland), equipped with a RF6 head. The nebulizer was placed outside the chamber and was connected with tubing with the RF6 head through a valve and a HEPA filter (with a diameter of 5.5 cm). For aerosol generation, about 0.1 g of the sample was placed in the bottom of the head. The sample was slowly evacuated from the head with the air flow from the nebuliser. Aerosol generation time was 30-60 s. The RF6 head was placed 0.65 m above the bottom surface of the chamber. Samples of BG spores were aerosolized inside the chamber at  $3.2 \times 10^5$  Pa pressure, an airflow rate of 15.5 l/min. Four VDC-001 Life-Desktop USB fans (0.14 m diameter, Veho, Eastleigh, Hampshire, UK) were used to stir air inside the chamber. The fans were situated along the diagonals of the chamber, 0.20 m above the bottom of the chamber. This arrangement was used to cut down on fast gravitational settling of the aerosolized BG endospores during experiments (Fig. 1). After each trial, the chamber was decontaminated with PeraSafe (Antec International DuPont, Sudbury, Suffolk, UK) and rinsed with water. Before each experiment, a UVC lamp (Puritec LPS9; OSRAM, GmGH, Augsburg, Germany) was switched on inside the chamber for 1 h. Then, interior air was exchanged through a HEPA filtration system for 30 min. All trials were conducted at room temperature (20 to 23°C).

## 2.5. Scanning Electron Microscopy

The SEM pictures were performed using Tescan Vega II SBU in a vacuum using SE detector. A carbon conductive strip with pollen grains was attached to SEM aluminium stub. Pollen grains were coated with about 20-nm thick gold layers. The thin layer of gold had no effect on the shape of the observed pollen. The sputtering was performed using Emitech K550X device.

## 2.6. Epifluorescence Microscopy

The reference suspensions of vegetative cells of the species *M. luteus* and *B. atrophaeus* endospores (BGs) were stained with fluorescent dyes. Two fluorescent stains were used: DAPI (for nucleic acid staining), SYTO-9 (5 mM) and propidium iodide (0.9 mM). SYTO-9 labelled alive bacterial cells, which fluoresce green; and propidium iodide labelled bacterial cells with compromised membranes that fluoresce red. The procedure of staining of *B. atrophaeus* endospores was performed according to Laflamme et al. (18). Then, labelled bacterial suspensions were filtered through polycarbonate membrane filters (Invitrogen) of a diameter of 25 mm, and a pore size of 0.22  $\mu\text{m}$  with using a filtration apparatus (Millipore). Filters were dried on microscope slides for 12 hours at room temperature and then mounted on slides using immersion oil for epifluorescence (BacLight mounting oil, Invitrogen). Filters were viewed under the epifluorescence microscope (Eclipse E 200, Nikon),

using a suitable filter for DAPI (EX330-380, DM400, BA420), SYTO-9 (FITC filter EX450-490, DM505, BA520) and propidium iodide (Rohamaine filter EX510-560, DM575, BA590). Microphotographs were taken with a Nikon DS-Fi1-U2 camera, using NIS-Elements F3.0 Nikon software.

## 2.7. Data analysis

Data analysis was performed in four steps. Firstly, graphical aerosol “fingerprints” were analysed visually on 3D diagrams (Particle diameter vs. Asymmetry factor vs. Particle number), and assigned to dissemination periods marked during the experiments. Secondly, the chosen samples were exported to ASCII file. The third step of data analysis included its preparation in MS Excel format in such a way that data matrix of  $40 \times 20$  cells (particle size  $\times$  asymmetry factor) was converted into one column of 800 rows. Individual data collected during the intervals formed separate columns. The data was analysed statistically using Hierarchical Cluster Analysis (HCA) (Statistica 10, StatSoft, Poland). The results of the HCA are shown as a dendrogram, which lists all of the samples in the form of clusters. The samples, which show similarity, are grouped in the same cluster and then any two clusters revealing similarity between each other are joined together. To indicate at what level of similarity any two clusters are joined, the distance between objects was measured using  $r$  Pearson correlation index. Ward’s method was used for clustering. In short, this method attempts to minimize the Sum of Squares of any two (hypothetical) clusters that can be formed at each step. On the  $y$ -axis of the dendrogram there is a result of Ward’s method named as a linkage distance, which is the measure of similarity between groups of objects. The largest similarity was ascribed to the value close to zero.

## 3. Results and discussion

The exemplary characteristics recorded with the use of ASPECT instrument and adequate SEM pictures of aerosolized particles are presented in the figures below. Figure 2 shows latex microspheres of various sizes ranging from 3 to 8  $\mu\text{m}$ . There was a good agreement between particle size distribution and diameters measured with SEM. Similarly, very low  $A_f$  values measured with ASPECT indicated spherical shape of the particles.

It has been shown that smut spores are dimpled spheres (19). Figure 3b revealed their cylindrical shape and resemblance to the red blood cells. In a wet environment, microorganisms and pollens tend to swell. The SEM pictures presented partially collapsed particles due to dry storage conditions. The  $A_f$  determined with ASPECT showed that JONs particles were far more heterogeneous than spherical standard

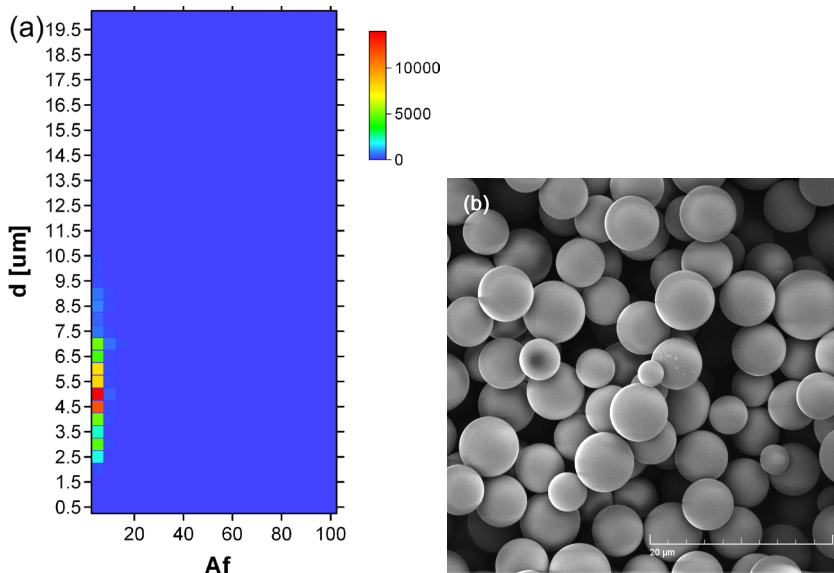


Fig. 2. Latex microspheres (PLS): a) particle size and shape distribution measured with ASPECT; b) SEM image

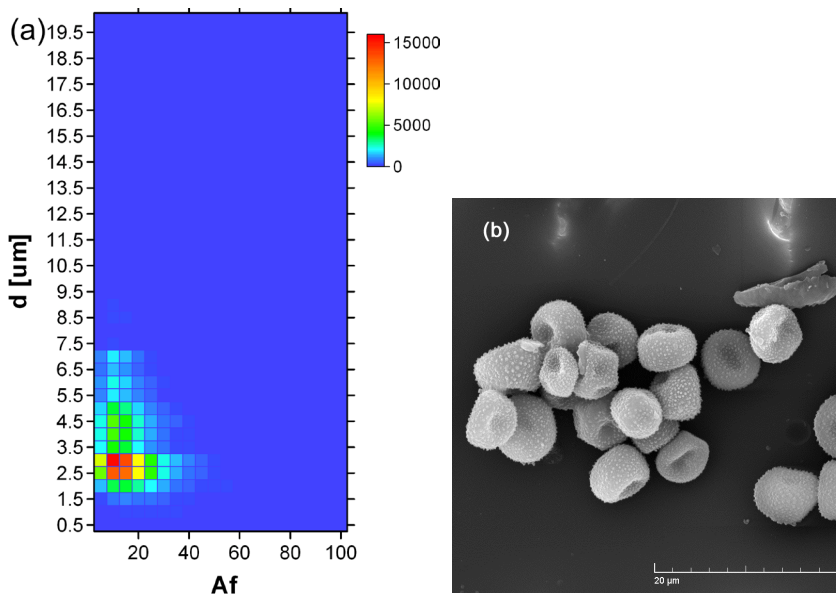


Fig. 3. Johnsons Grass Smut spores (JONS): a) particle size and shape distribution measured with ASPECT; b) SEM image

latex particles. Nevertheless, considerable fraction of almost spherical particles (Af 10-15) was detected. The JON's particles presented on SEM image were 4-7  $\mu\text{m}$  in diameter. Slightly wider particle size distribution (2-7  $\mu\text{m}$ ) has been recorded with optical scattering measurements. It also showed the highest concentration of particles with diameter 2.5-3.0  $\mu\text{m}$ .

The Ragweed pollen presented on SEM showed quite uniform spheres of 15-20  $\mu\text{m}$  in diameter (Fig. 4b). The ASPECT analysis presented in Figure 4a displayed broader dispersion of particle size and Af. However, it showed that considerable fraction of RAG particles exhibit their actual shape and size. Considering very good correlation between SEM and ASPECT for latex microspheres (Fig. 2), the light scattering on particles accurately determined the aerosol properties. However, the ASPECT data for RAG revealed a number of particles of 1-3 and 5-14  $\mu\text{m}$  diameter. They also presented diversified Af ranging from 0 to 60 Figure 4a. The discrepancy between SEM and ASPECT could arise from particle disruption in fast airflow (20). That effect could be possible at the aerosol generator as well as inside of the ASPECT nozzle. In order to check if aerosol generation destroys the RAG pollen grains, the particles were collected on the filter placed just at the aerosol generator nozzle mouth. The SEM pictures of the stock and filter collected particles were compared; however, they did not reveal any change in particle shape and fragmentation level (data not shown).

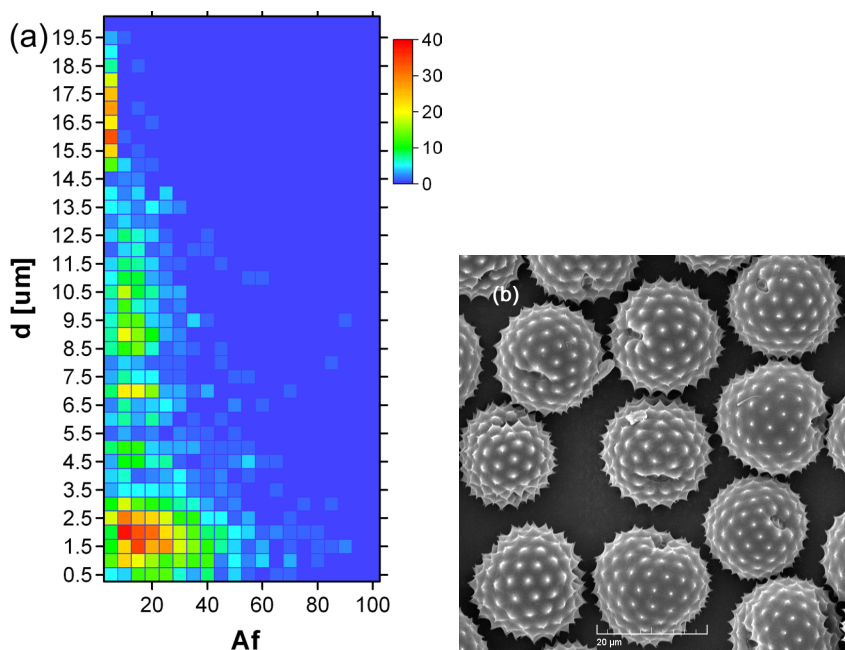


Fig. 4. Ragweed pollen (RAG): a) particle size and shape distribution measured with ASPECT; b) SEM image

Therefore, we can assume that fragmentation of the pollen grains occurs inside of the ASPECT device during the measurement process. Since the ASPECT device is a closed construction we do not know a method to capture particles which passed through the instrument's nozzle.

The Turex is an insecticide containing *Bacillus thuringiensis* spores. The SEM image of BTst represented particles of greatly diversified sizes and shapes (Fig. 5b). A broad distribution of Af and particle sizes measured by ASPECT correctly characterized diverse structures existing in the BTst preparation (Fig. 5a). The similar irregular pattern was observed also for technical *Bacillus atrophaeus* (BGst) — data not shown.

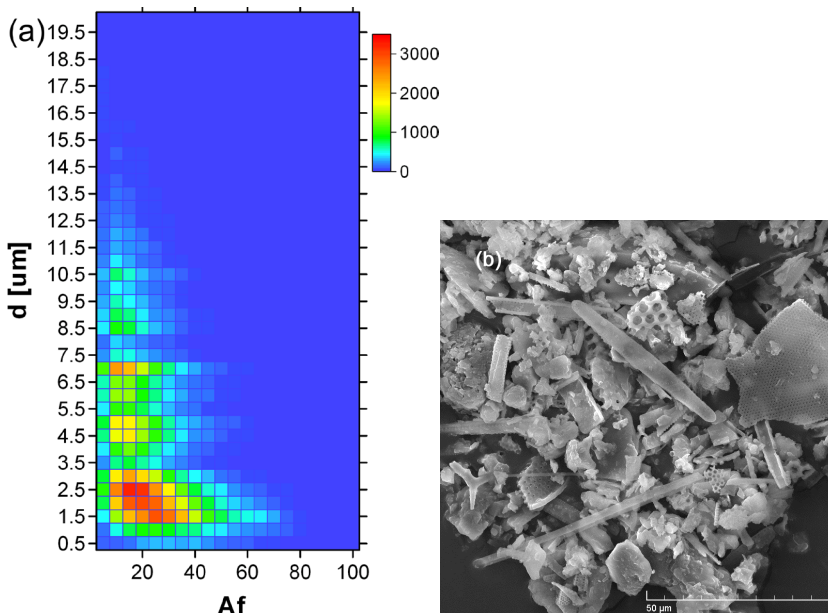


Fig. 5. Turex (BTst): a) particle size and shape distribution measured with ASPECT; b) SEM image

The *Micrococcus luteus* (Fig. 6a) and *Bacillus atrophaeus* spores (Fig. 7a) showed quite similar patterns regarding Af and particle size distribution. For both microorganisms, the maximum particle counts at diameters about 1.5-2.0 µm and Af around 30 were observed. The epifluorescence microscopy images (Fig. 6b and 7b) showed that single cell size was 1.2 and 1.4 µm for ML and BGs, respectively. Figure 6b clearly illustrated that ML occurs mainly as multicellular aggregates. Figures 8a and 8b presents normalized and percent distributions of particle Af regardless of their sizes. The ML displayed the broadest Af distribution comparing to other investigated aerosols that demonstrated strong aggregation of the bacteria (Fig. 6a).

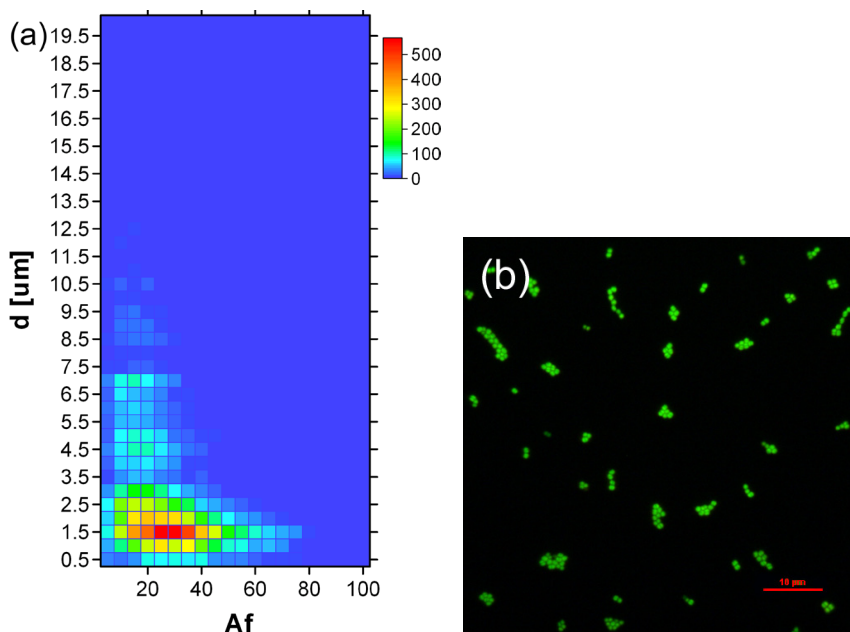


Fig. 6. *Micrococcus luteus* (ML): a) particle size and shape distribution measured with ASPECT; b) Fluorescence microscope image

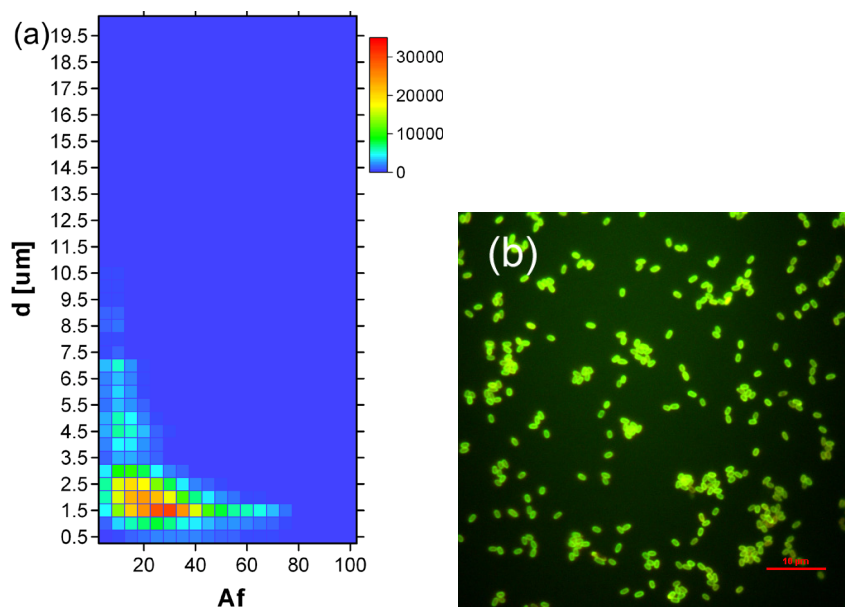


Fig. 7. *Bacillus atrophaeus* spores (BGs): a) particle size and shape distribution measured with ASPECT; b) Fluorescence microscope image

About 90% of PLS presented Af values close to zero that clearly define their spherical shapes (Fig. 8b). Similarly, bulk fraction of RAG particles displayed spherical shape that was reflected in Af values between 0 and 10 (Fig. 8b). The aerosol generated from JONs demonstrated maximum particle number of Af about 10, however about 10% of particles presented Af close to zero (Fig. 8b). The bacteria in aerosols (BGs, ML) formed elongated agglomerates also Turex consisted of a lot of long particles that was reflected in Af ranging from 10 to 60 (Fig. 5b and 8).

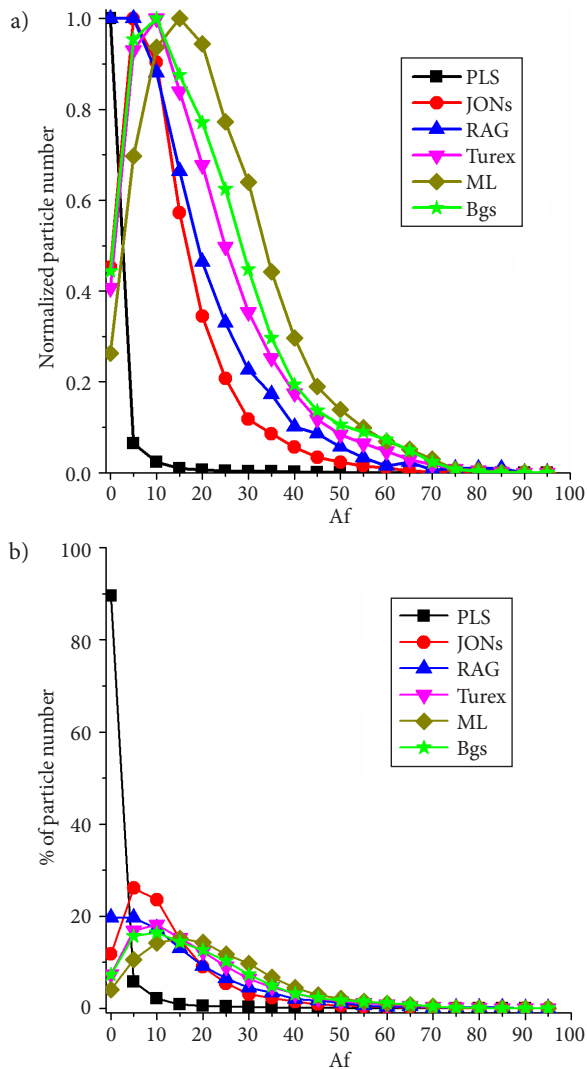


Fig. 8. a) Normalized number of particles of all sizes regarding Asymmetry factor (the number of particles of all sizes is summarized in bins of Af); b) percent of particles of given Af

The ASPECT detector recorded data as a particle diameter vs. Af matrices. Each type of aerosol produces specific distribution of particles. The classification of aerosols using Hierarchical Cluster Analysis (HCA) was successfully applied previously (11). Figure 9 demonstrated classification of various bioaerosols using HCA. As presented in the diagram, bacteria and spores formed separate clusters comprising technical and washed samples. A very close relationship was observed for technical spores BTst and BGst. Two samples of BTst (BTst-1 and BTst-2), aerosolized during different experiments, showed the highest similarity among all the samples that proved high fidelity of optical scattering techniques. The particle size vs Af matrices (Fig. 6 and 7) as well as dendrogram (Fig. 9) demonstrated similarity between washed BGs and ML. The pollens, RAG and PAP, formed separate cluster indicating that this group could be easily distinguished from bacteria and spores. The PLS, as the only artificial material, was assigned to the cluster entirely different from other examined substances.

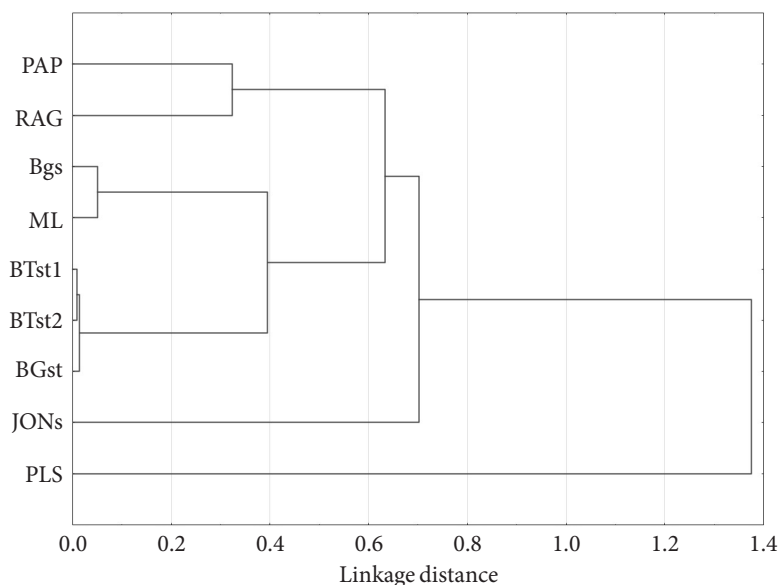


Fig. 9. Hierarchical Cluster Analysis

## 4. Conclusions

The ASAS technology accurately describes size and shape of aerosol particles. It was particularly noticeable for spherical standard (PLS) which presented high convergence between SEM images and optical properties. The pollens were accurately classified; however, there was a fraction of very small particles that was not adequate to actual characteristics of the particles presented on the SEM picture. Such wide

particle size and Af distribution may be due to the forces in the flowing air in the thin nozzle that were disruptive and possibly teared them off or released smaller fractions. This study has demonstrated that HCA offers fast and reliable bioaerosol classification based on shape and size data matrices of aerosols. The process can be automated for real time and continuous work. Introduction of real-time optical methods connected with statistical analysis could significantly improve environmental monitoring and aerosol characterization.

*Received February 1, 2017. Revised March 8, 2017.*

The presented work was supported by the grant from, “Development of Cluster of Biomedical Engineering Centre” co-financed by the European Union under the Operational Programme Innovative Economy. Task No. 3 (POIG.05.01.00-00-013/12-00).

#### LITERATURE

- [1] O’CONNOR DAVID J., et al., *Using the the WIBS-4 (Waveband Integrated Bioaerosol Sensor) Technique for the On-Line Detection of Pollen Grains*, *Aerosol Sci. Technol.*, vol. 48, 4, 2014, pp. 341-349.
- [2] TAKETANI FUMIKAZU, et al., *Measurement of fluorescence spectra from atmospheric single submicron particle using laser-induced fluorescence technique*, *J. Aerosol. Sci.*, vol. 58, 2013, pp. 1-8.
- [3] MITSUMOTO KOTARO, et al., *Development of a novel real-time pollen-sorting counter using species-specific pollen autofluorescence*, *Aerobiologia*, vol. 96, 2, 2010, pp. 99-111.
- [4] PAN YONG-LE, HUANG HERMES and CHANG RICHARD K., *Clustered and integrated fluorescence spectra from single atmospheric aerosol particles excited by a 263- and 351-nm laser at New Haven CT and Adelphi MD*, *J. Quant. Spectrosc. Radiat. Transfer*, vol. 113, 17, 2012, pp. 2213-2221.
- [5] PAN YONG-LE, et al., *Dual-excitation-wavelength fluorescence spectra and elastic scattering for differentiation of single airborne pollen and fungal particles*, *Atmos. Environ.*, vol. 45, 8, 2011, pp. 1555-1563.
- [6] PÖHLKER C., HUFFMAN J.A. and PÖSCHL U., *Autofluorescence of atmospheric bioaerosols — fluorescent biomolecules and potential interferences*, *Atmos. Meas. Tech.*, vol. 5, 2012, pp. 37-71.
- [7] JIM HO, MELVIN SPENCE and PETER HAIRSTON, *Measurement of biological aerosol with a fluorescent aerodynamic particle sizer (FLAPS): correlation of optical data with biological data*, *Aerobiologia*, vol. 15, 4, 1999, pp. 281-291.
- [8] KANAANI HUSSEIN, HARGREAVES MEGAN, SMITH JIM, RISTOVSKI ZORAN, AGRANOVSKI VICTORIA, MORAWSKA LIDIA, *Performance of UVAPS with respect to detection of airborne fungi*, *J. Aerosol Sci.*, vol. 39, 2, 2008, pp. 175-189.
- [9] FEUGNET GILLES, et al., *Improved laser-induced fluorescence method for bio-attack early warning detection system*, *Proc. of SPIE, Optically Based Biological and Chemical Detection for Defence IV*, 2008, p. 71160.
- [10] PAN YONG-LE, et al., *Fluorescence spectra of atmospheric aerosol particles measured using one or two excitation wavelengths: Comparison of classification schemes employing different emission and scattering results*, *Opt. Express*, vol. 18, 12, 2010, pp. 12436-12457.
- [11] KALISZEWSKI M., et al., *A new approach to UVAPS data analysis towards detection of biological aerosol*, *J. Aerosol Sci.*, vol. 58, 2013, pp. 148-157.

- [12] KAYE P.H., et al., *A real-time monitoring system for airborne particle shape and size analysis*, J. Geophys. Res., vol. 101, D14, 1996, pp. 19215-19221.
- [13] KAYE PAUL H., *Spatial light-scattering analysis as a means of characterizing and classifying non-spherical particles*, Meas. Sci. Technol., vol. 9, 2, 1998, pp. 141-149.
- [14] SZYMANSKI WLADYSLAW W.W., NAGY ATTILA and CZITROVSKY ALADÁR., *Optical particle spectrometry — Problems and prospects*, J. Quant. Spectrosc. Radiat. Transfer, vol. 110, 11, 2009, pp. 918-929.
- [15] JUNG JAE HEE and LEE JUNG EUN., *In situ real-time measurement of physical characteristics of airborne bacterial particles*, Atmos. Environ., vol. 81, 2013, pp. 609-615.
- [16] HO J. and DUNCAN S., *Estimating aerosol hazards from an anthrax letter*, J. Aerosol Sci., vol. 36, 5-6, 2005, pp. 701-719.
- [17] LEWANDOWSKI R., et al., *Use of a foam spatula for sampling surfaces after bioaerosol deposition*, Appl. Environ. Microbiol., vol. 76, 3, 2010, pp. 688-694.
- [18] LAFLAMME C., et al., *Assessment of bacterial endospore viability with fluorescent dyes*, J. Appl. Microbiol., vol. 96, 4, 2004, pp. 684-692.
- [19] BROCKMANN J.E. and RADER D.J., *APS Response to Nonspherical Particles and Experimental Determination of Dynamic Shape Factor*, Aerosol Sci. Technol., vol. 13, 2, 1990, pp. 162-172.
- [20] Visez Nicolas, et al., *Wind-induced mechanical rupture of birch pollen: Potential implications for allergen dispersal*, J. Aerosol Sci., vol. 89, 2015, pp. 77-84.

M. KALISZEWSKI, E.A. TRAFNY, M. WŁODARSKI, R. LEWANDOWSKI,  
M. STĘPIŃSKA, M. KWAŚNY, J. KOSTECKI, K. KOPCZYŃSKI

### **Analiza i klasyfikacja bioaerozoli w czasie rzeczywistym w oparciu o właściwości rozpraszania światła**

**Streszczenie.** Rozmiar i kształt cząstek biologicznych są ważnymi parametrami pozwalającymi na rozróżnianie pomiędzy różnymi rodzajami cząstek. Przeprowadzone zostały badania aerozoli pochodzenia biologicznego takich jak pyłki roślin, przetrwalniki oraz wegetatywne bakterie. Substancje te wykazywały różne właściwości morfologiczne. W wyniku przeprowadzonych badań przy pomocy optycznego analizatora wielkości i kształtu cząstek znaleziona została wysoka korelacja pomiędzy właściwościami rozpraszania światła a rzeczywistymi właściwościami cząstek, określonymi na podstawie SEM (Skaningowego Mikroskopu Elektronowego) oraz mikroskopu fluorescencyjnego. Przedstawione badania pokazują, że HCA (*Hierarchical Cluster Analysis*) umożliwia szybką, wiarygodną, prowadzoną w sposób ciągły analizę i klasyfikację bioaerozoli w oparciu o ich charakterystyki rozproszeniowe.

**Słowa kluczowe:** klasyfikacja bioaerozoli, rozpraszanie, analiza wielkości i kształtu cząstek, wykrywanie bojowych środków biologicznych, hierarchical cluster analysis (HCA)

**DOI:** 10.5604/01.3001.0009.9475